Measurements Using an Electron Beam," CAL Rept. AN-2112-Y-1, Aug. 1968, Cornell Aeronautical Lab.

[14] Laufer, J., "Some Statistical Properties of the Pressure Field Radiated by a Turbulent Boundary Layer," *The Physics of Fluids*, Vol. 7, No. 8, Aug. 1964.

[15] Kistler, A. L., "Fluctuation Measurements in a Supersonic Turbulent Boundary Layer," *The Physics of Fluids*, Vol. 2, No. 3, May–June 1959, pp. 290–296.

[16] Shaw, R., "The Influence of Hole Dimensions on Static Pressure Measurements," *Journal of Fluid Mechanics*, Vol. 7, 1960, pp. 550–564.

[17] Rainbird, W. J., "Errors in Measurement of Mean Static Pressure of a Moving Fluid Due to Pressure Holes," *Quarterly Bulletin 3*, 1967, National Research Council of Canada, National Aeronautical Establishment, pp. 55–89.

[18] Scaggs, N. E., "Boundary Layer Profile Measurements in Hypersonic Nozzles," Rept. 66-0141, July 1966, Aerospace Research Lab., U. S. Air Force.

[19] Speaker, W. V. and Ailman, C. M., "Spectra and Space-Time Correlations of the Fluctuating Pressures at a Wall Beneath a Supersonic Turbulent Boundary Layer Perturbed by Steps and Shock Waves," CR-486, May 1966, NASA.

[20] Coles, D., "Measurements in the Boundary Layer on a Smooth Flat Plate in Supersonic Flow," thesis, May 1953, California Inst. of Technology, Pasadena, Calif.

[21] Maddalon, D. V. and Henderson, A., Jr., "Boundary-Layer Transition on Sharp Cones at Hypersonic Mach Numbers," *AIAA Journal*, Vol. 6, No. 3, March 1968, pp. 424–431.

[22] Everhart, P. E. and Hamilton, H. H., "Experimental Investigation of Boundary-Layer Transition on a Cooled 7.5° Total-Angle Cone at Mach 10," TN D-4188, Oct. 1967, NASA.

[23] Lobb, R. K., Winkler, E. M., and Persh, J., "NOL Hypersonic Tunnel No. 4 Results VII: Experimental Investigation of Turbulent Boundary Layers in Hypersonic Flow," Rept. 3880, March 1955, Naval Ordnance Lab., China Lake, Calif.

[24] Perry, J. H. and East, R. A., "Experimental Measurements of Cold Wall Turbulent Hypersonic Boundary Layers," Aeronautics and Astronautics Rept. 275 Feb. 1968, Univ. of Southampton.

[25] Lowson, M. V., "Pressure Fluctuations in Turbulent Boundary Layers," TN D-3156, Dec. 1965, NASA.

[26] Richards, E. J., Bull, M. K., and Willis, J. L., "Boundary Layer Noise Research in the U.S.A. and Canada—A Critical Review," Rept. 21, 766, Feb. 1960, Aeronautical Research Council.

[27] Shattuck, R. D., "Sound Pressures and Correlations of Noise on the Fuselage of a Jet Aircraft in Flight," TN D-1086, Aug. 1961, NASA.

[28] Belcher, P. M., "Predictions of Boundary-Layer Turbulence Spectra and Correlations for Supersonic Flight," presented at the Fifth International Acoustical Congress, Liege, Belgium, Sept. 1965.

[29] Coe, C. F., "Surface-Pressure Fluctuations Associated With Aerodynamic Noise," *Conference on Basic Aerodynamic Noise Research*, NASA SP-207, July 1969, pp. 409–424.

[30] Houbolt, J. D., "On the Estimation of Pressure Fluctuations in Boundary Layers and Wakes," Rept. 90, June 1966, Aeronautical Research Association of Princeton Inc. Princeton N.J.

[31] Pierce, H. B. and Mayes, W. H., "Description of Hypersonic Boundary-Layer Noise Flight Measurement Program," *Conference on Basic Aerodynamic Noise Research*, NASA SP-207, July 1969, pp. 337–343.

MAY 1971 AIAA JOURNAL VOL. 9, NO. 5

Generalized Aerodynamic Forces on a Flexible Plate Undergoing Transient Motion in a Shear Flow with an Application to Panel Flutter

E. H. Dowell*
Princeton University, Princeton, N. J.

A theoretical solution to the title problem is obtained. Unlike previous solutions in the literature, the present method allows for finite plate dimensions and continuously varying mean velocity and temperature profiles. A computer program has been developed to calculate the required aerodynamic forces for boundary-layer profiles. These forces are then employed in a nonlinear flutter analysis previously developed by the author. The theoretical flutter results are compared with the experimental data of Muhlstein, Gaspers, and Riddle and generally good agreement is obtained. Other physical problems to which the present aerodynamic analysis is relevant include, 1) stabilization of viscous boundary layers by flexible walls, 2) sound wave propagation through shear layers, and 3) shear layer effects on control surface aerodynamics at supersonic speeds.

Nomenclature

a = plate length, also speed of sound
b = plate width
c_p, c_v = specific heats
D = plate stiffness, also derivative operator
E = modulus of elasticity
$H_{mnpq}, I_{mnpq}, K_{mnpq}$ = aerodynamic influence functions
h = plate thickness
k = reduced frequency
K = $\omega[\rho_m(ha^4/D)]^{1/2}$; also aerodynamic kernel
M = Mach number
p = pressure
Q_{mnpq} = generalized aerodynamic force
q = $\rho_\infty U_\infty^2/2$ = dynamic pressure
R = $c_P - c_v$ = gas constant
T = temperature
t = time
u,v,w = fluid velocity components
U_∞ = air velocity
w_p = plate deflection
x,y,z = spatial variables, nondimensionalized by a (or b)
z_w = wall position, nondimensionalized by a
λ^* $\equiv (2qa^3/D)$ = nondimensional dynamic pressure
μ = $\rho_\infty\theta/\rho_m h$ = mass ratio
δ = boundary-layer thickness

Received October 26, 1970; revision received February 1, 1971. Work supported by NASA Grants NGR 31-001-146 and NGR 31-001-197.

* Associate Professor, Department of Aerospace and Mechanical Sciences. Member AIAA.

ρ = air density
ρ_m = plate density
ω = frequency
α = Fourier transform variable
γ = Fourier transform variable; also ratio of specific heats
ν = kinematic coefficient of viscosity

Subscripts

f = flutter
p = peak
∞ = freestream

Superscripts

$(\bar{})$ = mean
$(\hat{})$ = perturbation

1. Introduction

IT is now firmly established on experimental grounds that the adjacent fluid shear (boundary) layer can be of importance in modifying the flutter behavior of plates as a result of the recent experimental investigations by Muhlstein, Gaspers, and Riddle[1] and Gaspers, Muhlstein, and Petroff.[2] Earlier qualitative indications of this effect were provided by the experiments of Lock and Fung,[3] Hodson and Stocker,[4] and Asher and Brown.[5] Theoretical analyses of the boundary-layer effect have been made by Miles,[5] McClure,[7] Anderson and Fung,[8] Olson,[9] and Zeydel.[10] While each analysis has its own special assumptions and characteristics, all with the exception of Zeydel assume the plate to be infinitely long for purposes of determining the aerodynamic forces. This approximation is generally inadequate as had been discussed by Dowell and Voss.[11] Zeydel, on the other hand, accounts for finite length but assumes the boundary layer may be approximated by multilayers of potential flows following Anderson and Fung. Such an approximation does not allow for the continuously varying behavior of the velocity (and temperature) profiles. This approximation, though perhaps qualitatively correct, leads to substantial quantitative errors. This will be discussed subsequently in greater detail in the body of the text where it is shown how the present analysis may be reduced to that of Zeydel or Anderson and Fung as a special case. The formulations of Miles and Olson are essentially that of the present analysis, i.e., a shear flow model. In this model the continuously varying nature of the velocity profile is accounted for but no direct effects of viscosity are retained in the flow perturbations due to plate motion. McClure retained the effects of viscosity in the perturbations as well. Neither Miles, Olson, nor McClure accounted for finite plate dimensions in his aerodynamic analysis (though McClure subsequently accounted for finite dimensions in his structural model). Based on the present results (and again referring to the earlier discussion by Dowell and Voss) none of these earlier analyses are quantitatively accurate and only that of Zeydel (who provided no numerical results) may be qualitatively correct. Of course, the present analysis may also need to be improved for certain applications. In particular, the neglect of viscous effects on the perturbed flow should be examined. It would appear feasible to include such effects using the present methods.

Although the subsequent focus of the paper will be on the application of this new aerodynamic analysis to panel flutter, it should be mentioned that the potential application is much wider. Other topics to which the present aerodynamic analysis is relevant include: 1) stabilization of viscous boundary layers by flexible wall, e.g., see Refs. 12 and 13; 2) sound (pressure) wave propagation through shear flows, e.g., sonic boom propagation through the Earth's shear layer or noise propagation through a boundary or jet shear layer, Ref. 14; 3) shear layer effects on control surface aerodynamics at supersonic speeds; 4) generation of water waves by shear flows (Miles' analysis of this problem which parallels his panel flutter work should be mentioned here; see Ref. 15 plus references contained therein dating to 1957). An early version of this work was reported in Ref. 16. Certain improvements have been made in the present work as will be discussed subsequently.

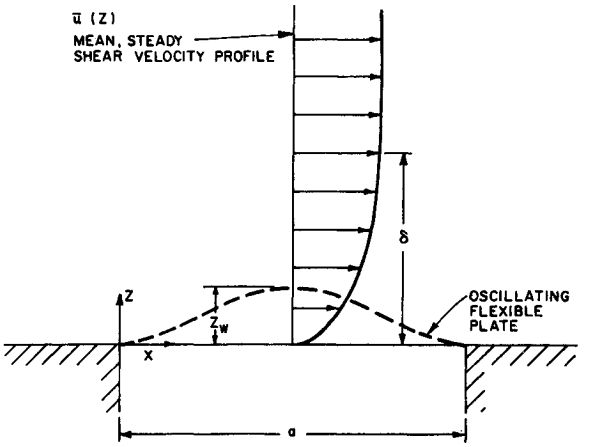

Fig. 1 Problem geometry.

2. Problem Formulation

2.1 Derivation of Governing Equation

We begin with the equations of mass, momentum, and energy as found, e.g., in Ref. 17. The flow will be divided into a mean and a perturbation. The mean flow may be determined by theory or experiment and includes directly the effects of viscosity. The direct effects of viscosity are neglected in the perturbation flow and viscosity only enters through the effect of the mean flow on the perturbation flow. To derive the perturbation equations it is sufficient to consider nonlinear, inviscid flow (see Fig. 1).

The continuity of mass equation reads

$$\partial\rho/\partial t + \partial(\rho u)/\partial x + \partial(\rho v)/\partial y + \partial(\rho w)/\partial z = 0 \quad (1)$$

The three momentum equations read:

$$\rho[\partial u/\partial t + u\partial u/\partial x + v\partial u/\partial y + w\partial u/\partial z] = -(\partial p/\partial x) \quad (2)$$

$$\rho[\partial v/\partial t + u\partial v/\partial x + v\partial v/\partial y + w\partial v/\partial z] = -(\partial p/\partial y) \quad (3)$$

$$\rho[\partial w/\partial t + u\partial w/\partial x + v\partial w/\partial y + w\partial w/\partial z] = -(\partial p/\partial z) \quad (4)$$

The energy equation reads:

$$\rho\{c_v(\partial T/\partial t + u\partial T/\partial x + v\partial T/\partial y + w\partial T/\partial z) + (\partial/\partial t + u\partial/\partial x + v\partial/\partial y + w\partial/\partial z)[(u^2 + v^2 + w^2)/2]\} = -[\partial(pu)/\partial x] - \partial(pv)/\partial y - \partial(pw)/\partial z \quad (5)$$

Finally, we have the perfect gas formulas

$$p = \rho RT \quad (6)$$

Assume

$$u = \bar{u}(z) + \hat{u}, \quad v = \hat{v}, \quad w = \hat{w}, \quad p = \bar{p}(z) + \hat{p}$$
$$\rho = \bar{\rho}(z) + \hat{\rho}, \quad T = \bar{T}(z) + \hat{T} \quad (7)$$

The mean flow quantities, $\bar{u},p,\bar{\rho},\bar{T}$ are only functions of z whereas the perturbation quantities $\hat{u},\hat{v},w,\hat{p},\rho,\hat{T}$ are functions of x,y,z,t. The mean flow quantities satisfy Eqs. (1–6) trivially but are nontrivial solutions to the full Navier-Stokes equations which include viscosity.

Using the boundary-layer approximation for the mean flow, we note that

$$\bar{p} = p_\infty \quad \text{since } \partial\bar{p}/\partial z = 0 \quad (8)$$

Thus

$$\bar{\rho}\bar{T} = \rho_\infty T_\infty \quad (9)$$

and from conservation of energy

$$c_p\bar{T} + \tfrac{1}{2}\bar{u}^2 = c_pT_\infty + \tfrac{1}{2}U_\infty^2 \tag{10}$$

where the subscript ∞ denotes freshstream values outside the boundary layer.

Using the thermodynamic relations $c_p - c_v = R, c_p/c_v = \gamma, a_\infty^2 = \gamma RT_\infty$ one may derive from Eq. (10)

$$\bar{T}/T_\infty = 1 + [(\gamma - 1)/2]M_\infty^2[1 - (\bar{u}/U_\infty)^2] \tag{11}$$

Thus if $\bar{u}$ is known from theory or experiment we may compute $\bar{T}$ from Eq. (11). One might also include a recovery factor for the temperature but calculations have shown this effect to be unimportant for the present purpose. To derive the equations for the perturbed flow, we substituted Eq. (7) into Eqs. (1–6). The result is (linearizing in the perturbed quantities)

$$\partial\hat{\rho}/\partial t + \bar{u}\partial\hat{\rho}/\partial x + \bar{\rho}[\partial\hat{u}/\partial x + \partial\hat{v}/\partial y + \partial\hat{w}/\partial z] + \hat{w}d\bar{\rho}/dz = 0 \tag{12}$$

$$\bar{\rho}[\partial\hat{u}/\partial t + \bar{u}\partial\hat{u}/\partial x + (d\bar{u}/dz)\hat{w}] = -\partial\hat{p}/\partial x \tag{13}$$

$$\bar{\rho}[\partial\hat{v}/\partial t + \bar{u}\partial\hat{v}/\partial x] = -\partial\hat{p}/\partial y \tag{14}$$

$$\bar{\rho}[\partial\hat{w}/\partial t + \bar{u}\partial\hat{w}/\partial x] = -\partial\hat{p}/\partial z \tag{15}$$

$$\bar{\rho}[c_v(\partial\hat{T}/\partial t + \bar{u}\partial\hat{T}/\partial x + \hat{w}d\bar{T}/dz)] = -\bar{p}[\partial\hat{u}/\partial x + \partial\hat{v}/\partial y + \partial\hat{w}/\partial z] \tag{16}$$

$$\hat{p}/\bar{p} = \hat{T}/\bar{T} + \hat{\rho}/\bar{\rho} \tag{17}$$

In Eq. (16), Eq. (13) has been used to cancel some terms and simplify the equation.

Equations (12–17) are a system of linear equations which may be reduced to a single equation for a single unknown. Here the unknown of interest is pressure and the equation

$$[M_\infty^2/(\bar{T}/T_\infty)]D^3\hat{p} - D\nabla^2\hat{p}U_\infty^2 + 2(\partial^2\hat{p}/\partial x\partial z)(d\bar{u}/dz)U_\infty^3 - D(\partial\hat{p}/\partial z)(1/\bar{T})(d\bar{T}/dz)U_\infty^2 = 0 \tag{18}$$

where $D \equiv \partial/\partial t + \bar{u}\partial/\partial x$.

Finally, we introduce nondimensional quantities

$$x \equiv x/a, \quad y \equiv y/b, \quad z \equiv z/a, \quad t \equiv tU_\infty/a$$
$$u \equiv \bar{u}/U_\infty, \quad p \equiv \hat{p}/\rho_\infty U_\infty^2, \quad T \equiv \bar{T}/T_\infty \tag{19}$$

and

$$D \equiv \partial/\partial t + u\partial/\partial x$$
$$\nabla^2 \equiv \partial^2/\partial x^2 + \partial^2/\partial z^2 + (a/b)^2\partial^2/\partial y^2 \tag{20}$$

Eq. (18) becomes

$$(M_\infty^2/T)D^3p - D\nabla^2p + 2(\partial^2p/\partial x\partial z)du/dz - D(\partial p/\partial z)(1/T)(dT/dz) = 0 \tag{21}$$

Rather than introduce yet more symbols we have returned to the original ones; this should cause no great difficulty.

We also will need a boundary condition at the wall in terms of pressure. The boundary condition in terms of velocity is (in dimensional terms and linearized)

$$\hat{w} = \partial w_p/\partial t + \bar{u}\partial w_p/\partial x \quad \text{on } z = z_w \tag{22}$$

where
$w_p \equiv$ plate deflection, $z_w \equiv$ wall position, subsequently to be identified with w_p. From Eqs. (15 and 22)

$$\partial\hat{p}/\partial z = -\bar{\rho}[\partial/\partial t + \bar{u}\partial/\partial x]^2w_p \tag{23}$$

Nondimensionalized,

$$\partial p/\partial z = -\rho[\partial/\partial t + u\partial/\partial x]^2w_p/a \quad \text{on } z = z_w \tag{24}$$

where now z_w is also nondimensionalized by a.

Equations (21) and (24), as nondimensionalized, are the ones we must solve. It is perhaps of interest to point out that the Anderson-Fung and Zeydel models are equivalent to setting $du/dz = dT/dz = 0$ in Eq. (21). Numerical results indicate omission of such terms leads to substantial quantitative errors.

2.2 Formal Mathematical Solution

The basic solution procedure, with two notable exceptions, is that used in Ref. 18. Fourier transforms are employed in x and y to reduce Eq. (21) to a partial differential equation in z, i.e., defining

$$p^* \equiv \int_{-\infty}^{\infty}\int pe^{-i\alpha x - i\gamma y}\,dxdy$$

Eq. (21) becomes an equation for p^* with parameters α and γ. This partial differential equation is further reduced to a system of ordinary differential equations in time by using a finite difference representation in z, i.e.,

$$p_i^* \equiv p^* \text{ at } z = i\Delta z$$
$$(\partial p^*/\partial z)_i \cong (p_{i+1}^* - p_{i-1}^*)/2\Delta z$$
$$(\partial^2 p^*/\partial z^2)_i \cong (p_{i+1}^* - 2p_i^* + p_{i-1}^*)/\Delta z$$

where Δz = difference increment, i = index running over all difference elements in z direction.

The values of u,T, etc., employed are those at the midpoint of each difference element. For brevity we do not write out this system of ordinary differential equations in time for p_i^*. The boundary condition Eq. (24), must be expressed in difference form too, of course. The resulting system equations may be integrated with respect to time to determine p_i^*. In the next section we shall discuss numerical techniques in more detail but for the present let us assume p_i^* can be obtained by numerical means.

If p_i^* is available we may proceed to a determination of generalized aerodynamic forces as follows.

Let us compute p_w^* for a step function change in (the Fourier Transform) of

$$\rho[\partial/\partial t + u_w\partial/\partial x]^2w_p/a$$

where

$$p_w^* = p^*, \quad u_w = u \qquad \text{at } z = z_w$$

Call this solution K; then the solution for any motion can be written as

$$p_w^*(\alpha,\gamma;t) = K'(\alpha,\gamma,t)[\partial/\partial t + i\alpha u_w]w_p^*(\alpha,\gamma;t)|_{t=0} + w_p^*(\alpha,\gamma;t)|_{t=0}[\partial/\partial t + i\alpha u_w]K'(\alpha,\gamma;t) + \int_0^t K'(\alpha,\gamma;t-\tau)\left[\frac{\partial}{\partial\tau} + i\alpha u_w\right]^2 w_p^*(\alpha,\gamma;\tau)d\tau \tag{25}$$

where

$$K' \equiv dK/dt(\alpha,\gamma;t) \tag{26}$$

and

$$w_p^* \equiv \int_{-\infty}^{\infty}\int w_pe^{-i\alpha x - i\gamma y}\,dxdy \tag{27}$$

Formally Eq. (25) may be inverted to obtain

$$p_w = \frac{1}{(2\pi)^2}\int_{-\infty}^{\infty}\int P_w^*e^{i\alpha x + i\gamma y}\,d\alpha d\gamma \tag{28}$$

but this is not very efficient.

For the usual applications, the forces of interest are the "generalized aerodynamic forces" rather than the pressure itself. If

$$w_p(x,y,t) = \sum_m\sum_n A_{mn}(t)\psi_m(x)\psi_n(y) \tag{29}$$

Then the nondimensional generalized force, Q_{mnpq}, is defined as

$$Q_{mnpq} \equiv \int_0^1 \int_0^1 p_{mn}\psi_p(x)\psi_q(y)dxdy \tag{30}$$

where p_{mn} is the (nondimensional) pressure due to

$$w_p/a = (A_{mn}/a)\psi_m\psi_n \tag{31}$$

A considerable economy of effort may be achieved by performing the integrals over x and y in Eq. (30) before inverting the transform in Eq. (28). Having done this, Q_{mnpq} may be written as:

$$Q_{mnpq} = H_{mnpq}(t)\frac{da_{mn}(0)}{dt} + [H_{mnpq}'(t) + 2I_{mnpq}(t)]a_{mn}(0) + \int_0^t \left[H_{mnpq}(t-\tau)\frac{d^2a_{mn}}{d\tau^2} + 2I_{mnpq}(t-\tau)\frac{da_{mn}}{d\tau} + K_{mnpq}(t-\tau)a_{mn}(\tau)\right]d\tau \tag{32}$$

where

$$H_{mnpq} \equiv (1/2\pi)^2 \int_{-\infty}^{\infty}\int K'G_{mnpq}d\alpha d\gamma$$

$$I_{mnpq} \equiv (1/2\pi)^2 u_w \int_{-\infty}^{\infty}\int K'i\alpha G_{mnpq}d\alpha d\gamma$$

$$K_{mnpq} \equiv (1/2\pi)^2 u_w{}^2 \int_{-\infty}^{\infty}\int K'(i\alpha)^2 G_{mnpq}d\alpha d\gamma$$

$$G_{mnpq} \equiv \int_0^1 \psi_m e^{-i\alpha x}dx \int_0^1 \psi_p e^{i\alpha x}dx \times \int_0^1 \psi_n e^{-i\alpha y}dy \int_0^1 \psi_q e^{i\gamma y}dy \tag{33}$$

Certain simplifications follow because of symmetry or antisymmetry with respect to α and γ, see Ref. 18.

Finally, we note that an analytical formulae is available for K' in the inviscid limit

$$K'(\alpha,\gamma;t) = (e^{-i\alpha t}/M)J_0\{[\alpha^2 + \gamma^2(a/b)^2]^{1/2}t/M\} \tag{34}$$

See Eq. (5), Ref. 18. This result is helpful in planning numerical procedures for the boundary-layer case.

The author's colleague, C. S. Ventres, has developed an alternate solution technique for K' which avoids the finite difference procedure. His solution is an analytical one based upon an expansion in terms of δ/a and the method of matched asymptotic expansions. This work will be published later.

2.3 Numerical Technique

It is not desirable to go into great detail concerning numerical technique since the methods used are not individually novel. However, it is perhaps of some general interest to motivate the combination of techniques chosen and describe birefly some of the difficulties encountered and overcome.

We need to effectively perform six integrations. Four of these are with respect to three spatial variables and time to determine p from Eq. (21). Two more are required to determine the generalized aerodynamic forces from Eq. (30) once p is known. The object of course is to minimize the number of numerical integrations (or maximize the number of analytical integrations). The present combination of techniques permits two of the integrations [effectively the ones required in Eq. (30)] to be done analytically, the remaining four requiring numerical procedures.

To review, in Eq. (21), the x and y variables are treated by Fourier transforms, the z variable by finite differences and time by one of the standard means of integration of initial value problems. The advantage of the Fourier transforms, is that, while they must be inverted by numerical integration, they do permit the integrals in Eq. (30) to be accomplished analytically. As far as can be determined this is the "best" one can do. One may recall that for the inviscid theory, it is possible to do the integrations in z and t analytically as well. So the complication of shear flow as far as numerical technique is concerned is to require two additional numerical integrations. Roughly speaking, each additional numerical integration increases the computer time by a factor of ten. Hence, in the shear flow model we have an increase in computation time by approximately a factor of one-hundred over the inviscid model.

Finally, we should point out that to insure accuracy and stability of the numerical integrations with respect to z and t certain restrictions must be observed. Since we are dealing (basically) with the wave equation, we require for numerical stability that (in nondimensional terms) the increments in z and t obey

$$\Delta z = C\Delta t/M \qquad \text{where } C > 1$$

We chose $C = 3$. Also Δt must be sufficiently small to represent K' accurately. Knowing K' for inviscid flow, Eq. (34), and by numerical experimentation, we normally used a value

$$\Delta t \simeq 0.01$$

2.4 Boundary Conditions

Plate boundary condition

This is an important approximation in the analysis. In the framework of linear aerodynamic theory (even with a nonuniform mean velocity profile) we normally apply the boundary not on the instantaneous body surface but rather on its fixed reference surface, i.e., in the present case $z_w = 0$. As will be seen subsequently, such an approximation is physically less acceptable for the present problem. The reason being that such an approximation overestimates the stabilizing effect of the boundary layer as a result of the fact that the mean velocity at $z_w = 0$ is zero, i.e., $u_w \equiv 0$.

To apply the boundary condition exactly on the instantaneous plate surface is, of course, difficult since we do not know a priori where the plate is. That is, as yet, the plate motion is undetermined. Therefore, we adopt an approximation of the exact boundary condition based on a physically plausible hypothesis. We assume a nonzero value of z_w and determine from a (nonlinear) flutter analysis the plate deflection vs dynamic pressure, say. From such flutter results only a single value of plate deflection (corresponding to a single dynamic pressure) will be compatible with out assumed z_w. However, by repeating the calculation for several z_w we may determine the complete graph of plate deflection vs dynamic pressure.

It should be pointed out that there is still some ambiguity in this compatibility condition as the plate deflection continuously varies with space and time. Here we choose to equate the (maximum) center plate deflection to z_w. Other choices could be made, of course, e.g., some average value such as the root mean square. Fortunately, as we will see, the results are not very sensitive to the precise deflection chosen. This same difficulty has been faced by Benjamin[12] and Miles[15] in their analyses.

Boundary condition at "infinity"

There is another boundary condition which must be applied far away from the body. For convenience in the numerical work we place a rigid wall above the flexible plate sufficiently far away so that no waves are reflected back onto the plate. This boundary condition offers no special difficulty.

2.5 Brief Critique of the Basic Assumptions

Implicit in the analysis is the assumption that the *mean* (boundary layer) shear flow is unaffected by the panel motion. This will be a reasonable assumption when the panel ampli-

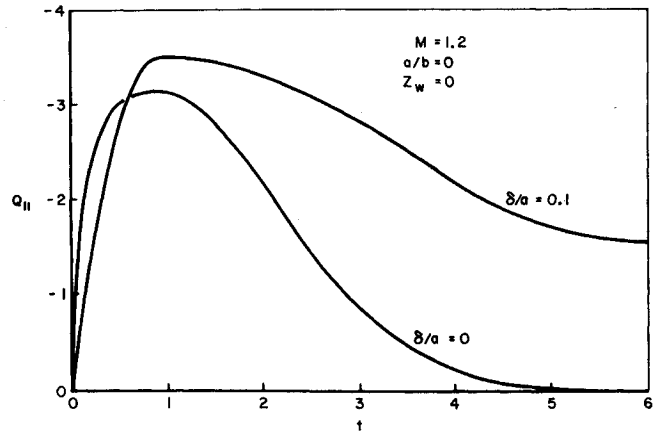

Fig. 2 Generalized aerodynamic force vs time.

tude is small compared to the boundary-layer thickness and hence the shear flow has a significant effect. It may not be a reasonable assumption when the panel amplitude is on the order of or larger than the boundary-layer thickness, but in those cases the shear layer effect is small. Hence, the assumption is best where the analysis is most needed.

One can also examine the relative time or frequency scales of the panel oscillation as compared to those of the boundary layer. If the motion of the panel is rapid relative to the characteristic frequencies of the boundary layer, then again the boundary layer should be unresponsive. In some sense this will always be true for the mean flow component (zero frequency) of the boundary layer. Even if one examines the characteristic response time of the boundary-layer flow, δ^2/ν, one concludes that the panel motion is generally rapid relative to that of the boundary layer.

Another basic assumption of the analysis is that the boundary-layer thickness is constant along the plate chord. Again this will be satisfactory for thicker boundary layers (where the boundary-layer effect is important) but less so for thinner ones (where there is a lesser effect).

Nevertheless, it should be emphasized that the success of what in its basic ingredients is a simple model makes for a rather pleasant surprise. The previous remarks may explain in part the success of the theoretical model.

3. Discussion of Results

In this section, results are given of both a purely aerodynamic nature as well as from flutter analysis. The method of flutter analysis used is essentially that of Ref. 19 and as modified and extended by Ventres.[20] Formally the aerodynamic generalized forces may be expressed as

$$Q_{mnpq} = Q_{mnpq}(t;M,a/b,\delta/a,z_w)$$

where a particular set of plate model functions and a particular mean velocity profile shape are implied. The (peak) plate deflection and frequency of oscillation may be expressed as:

$$(w_p/h)_p = (w_p/h)_p(x,y;\lambda^*,\mu,M,a/b,\delta/a,a/h)$$

$$K = K(\lambda^*,\mu,M,a/b,\delta/a,a/h)$$

As will be seen the explicit dependence on a/h is fairly weak. A one-seventh power law is used to approximate the mean velocity profile

$$\bar{u} = (z/\delta)^{1/7}$$

except as noted.

3.1 Aerodynamic Results

The first step in a flutter solution is to generate the required aerodynamic forces using the analysis of Sec. 2. That is, for a given boundary-layer (outer) thickness, δ/a, and a given wall displacement, z_w, the aerodynamic forces may be determined for various Mach number and plate aspect ratio or length/width ratio. From the point of view of flutter behavior the aerodynamic generalized forces are the most useful. In Figs. 2 and 3, we present the generalized forces Q_{11} (work done on first mode due to first mode deformation) and Q_{12} (work done on second mode due to first mode deformation) for a unit step function in the first mode. These results are for a two-dimensional plate at $M = 1.2$, $\delta/a = 0.1$ and $z_w = 0.01$. Also shown for comparison are results for inviscid flow, $z_w \geq \delta/a = 0$. The initial condition terms have been omitted, $a_1(0) = \dot{a}_1(0)$; these terms are normally unimportant for flutter. Hence, the results shown are essentially the integrals of K_{mnpq}. As may be seen the largest differences between boundary-layer and inviscid flow are for t large for Q_{11}, for t small for Q_{12}. In the frequency domain, t small and t large correspond to large and small frequency, respectively. Anticipating the relative small (reduced) frequency of the flutter oscillation we expect that Q will be more significantly effected by the boundary layer for flutter. It should be noted that with a (subsonic) boundary layer the memory of the fluid, in principle, becomes infinite. In practice there is little increase in the duration of the flow memory.

It is well known that for the inviscid theory at $M = 1.2$ the flutter is of a single-degree-of-freedom type due to negative aerodynamic damping in the first mode. This is most informatively examined by considering the aerodynamic force Q_{11} due to sinusoidal motion in the first mode. In the inviscid results, Q_{11} is negative for a range of $k = 0 \rightarrow 0.72$ indicating negative aerodynamic damping. Results obtained (not shown) for a small boundary-layer thickness, $\delta/a = 0.05$, demonstrate that the range of k for which negative aerodynamic damping can occur is reduced and for the larger boundary layer, $\delta/a = 0.1$, it is virtually eliminated. This further suggests that Q_{11} will be more strongly affected than Q_{12} by the boundary layer. For the flutter analyst it also indicates that single-degree-of-freedom flutter which is governed by Q_{11} and occurs at low, supersonic Mach number ($M < 1.4$ roughly) will be more significantly affected by the boundary layer than the well-known coalescence or merging frequency flutter which is governed largely by Q_{12} and occurs at the higher supersonic Mach number. This, of course, agrees with available experimental evidence.[1,2]

3.2 Flutter Results

We now turn to a discussion of flutter per se. The procedure will be briefly reviewed first. For a given δ/a and z_w (also fixed Mach number and aspect ratio) the aerodynamic forces are generated as above. These are then employed in a nonlinear flutter analysis similar to that described in Ref. 19 and as modified by Ventres[20] to account for clamped edge conditions. The clamped edge condition is selected in order

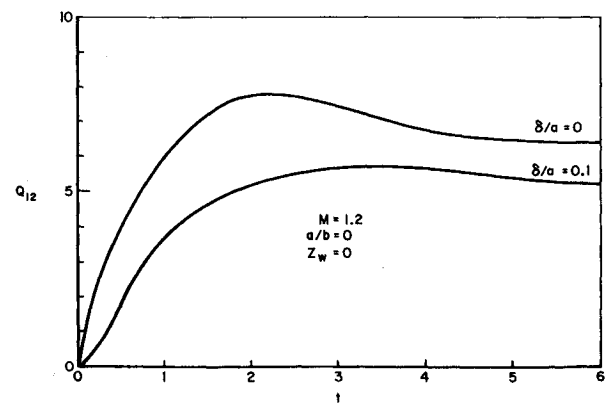

Fig. 3 Generalized aerodynamic force vs time.

to make a subsequent quantitative comparison with available experimental data. The results of such calculations are shown in Fig. 4 in the form of plots of (nondimensional) plate deflection (at the plate center) vs (nondimensional) dynamic pressure for various z_w and $\delta/a = 0.1$ Now as a result of the requirement that the plate deflection be identified with the wall displacement, z_w, of the aerodynamic analysis, only one point on each curve is physically compatible. That is

$$az_w = (w_p/h)_p h, \quad \text{or} \quad (w_p/h)_p = (a/h)z_w$$

at some selected plate position. Here we choose the center of the plate which corresponds to approximately the maximum plate deflection. Some other criterion could be used such as average plate deflection, however the use of the maximum w_p/h is conservative in that it (slightly) underestimates what we will see to be the stabilizing effect of the boundary layer.

Employing the compatibility condition between the aerodynamic and flutter analyses we may obtain a physically meaningful plot of plate deflection versus dynamic pressure for fixed δ/a. In Fig. 5, such results are shown for $\delta/a = 0.1$ using the above compatibility condition and also for $z_w \equiv 0$, i.e., the usual linear aerodynamic boundary condition. In addition, results are given for no boundary layer, the inviscid theory.

The most interesting part of Fig. 5 is the indication that the lowest dynamic pressure at which a flutter oscillation can occur is for a finite plate deflection when the most refined theory is used. That is, an analysis which considered only infinitesimal disturbances in a linear stability analysis would overestimate the increase in flutter dynamic pressure due to boundary-layer effects. We also note that it is highly probable that the lower part of the stability boundary is the dividing line between stable and unstable disturbance magnitudes. Below it, disturbances decay; above it, disturbances grow to the upper boundary. This is not proven, however. In any event, the quantitative effect of the nonlinearities is not large as far as determining *flutter dynamic pressure*; hence, the approximation $z_w \equiv 0$ was used in the remaining results. Note the present results differ from earlier ones[16] due to improved modeling of the flow profile by finite differences, especially the use of the midpoint profile characteristics over each difference element.

Using results such as those in Fig. 5, we may make comparisons with available experimental data. Before doing so, however, we discuss results analogous to Fig. 5 for $M = 2$. Such results show that indeed the effect of the boundary layer at high Mach number, $M = 2$, (about 20% increase in flutter dynamic pressure) is much smaller than at low supersonic Mach number, $M = 1.2$, (about 300% increase in dynamic pressure, see Fig. 5).

All flutter results were obtained using two structural modes. At $M = 2$ this involves some quantitative error. However this is of no importance for the present purposes.

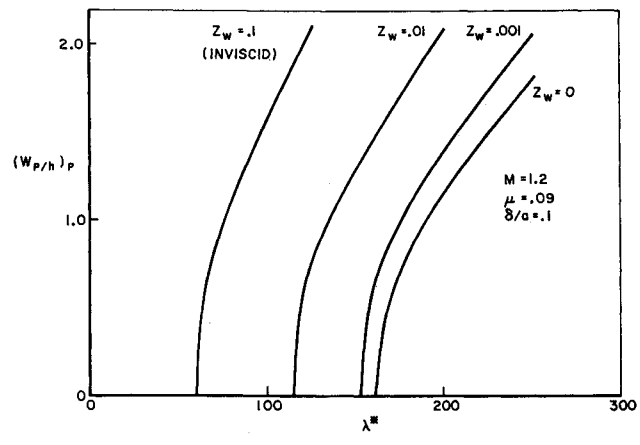

Fig. 4 Plate amplitude vs dynamic pressure.

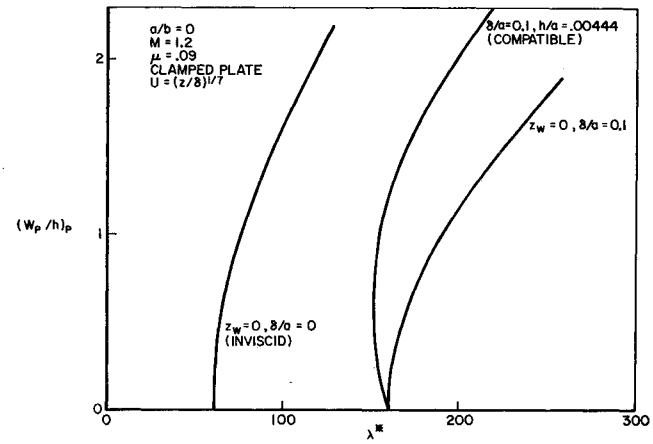

Fig. 5 Plate amplitude vs dynamic pressure.

3.3 Correlation of Theory and Experiment

Several investigators have noted qualitatively the effects of the boundary layer on panel flutter, the most recent and most thorough experiments are those of Muhlstein, Gaspers, and Riddle[1] and Gaspers, Muhlstein and Petroff.[2] In these experiments we have for the first time a quantitative measure of the boundary-layer effect. Previously the author[21] has compared the experimental data of Ref. 1 extrapolated to zero boundary-layer thickness with the results of inviscid theory. In general, good agreement was obtained over a range of Mach numbers, 1.1–1.4. Here we shall first focus on one Mach number, $M = 1.2$, which is thought to be representative and compare the results of the present analysis with the data of Ref. 1 for a range of boundary layer thicknesses. In Fig. 6, is shown flutter dynamic pressure vs boundary-layer thickness. For the plate in question, $h/a = 0.0044$. The mass ratio, μ, ranged from $\mu = 0.043$ to 0.09, see Fig. 6. The theoretical results are for a two-dimensional plate (length/width ratio, $a/b = 0$) and $a/b = 0.5$ while the experimental data are for a plate of length/width ratio, $a/b = 0.5$. As can be seen there is good agreement between theory and experi-

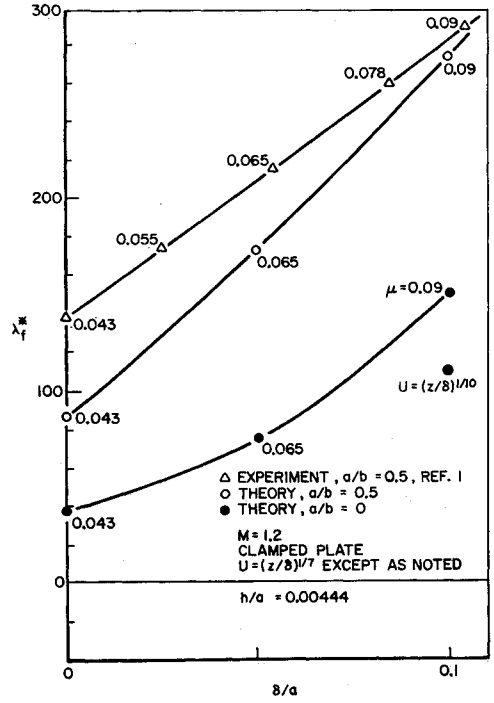

Fig. 6 Flutter dynamic pressure vs boundary-layer thickness.

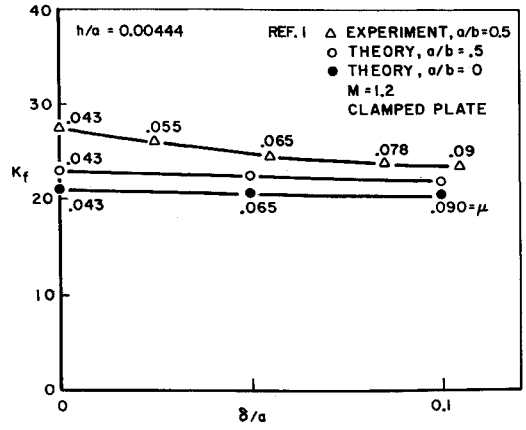

Fig. 7 Flutter frequency vs boundary-layer thickness.

ment with regard to trend and also reasonable quantitative agreement. In Fig. 7, we plot the flutter frequency versus boundary layer thickness and again the agreement is reasonable.

It should be mentioned that there is some change in flutter modal content with increasing boundary-layer thickness. Although the first natural mode of the plate dominates the flutter mode, there is an increase of second mode content relative to first mode content from roughly 15% for no boundary layer to 40% for $\delta/a = 0.1$. This clearly indicates the flutter motion is less of a single-degree-of-freedom type with a boundary-layer present.

We should also discuss the possibility of a single-degree-of-freedom instability in the second mode which the inviscid theory predicts is the most critical (occurs at the lowest dynamic pressure). In the experiments of Refs. 1 and 2 such an instability was not observed, instead the flutter mode was determined to be dominated by the first plate mode. The thinnest boundary layer achieved experimentally was $\delta/a \simeq 0.025$. Theoretical results indicate that even this extremely thin boundary layer is sufficient to completely suppress the second mode instability. Hence when the available experimental data[1,2] are extrapolated to zero boundary-layer thickness as is done here one should compare them with the inviscid theoretical results for the first rather than the second mode flutter.[21]

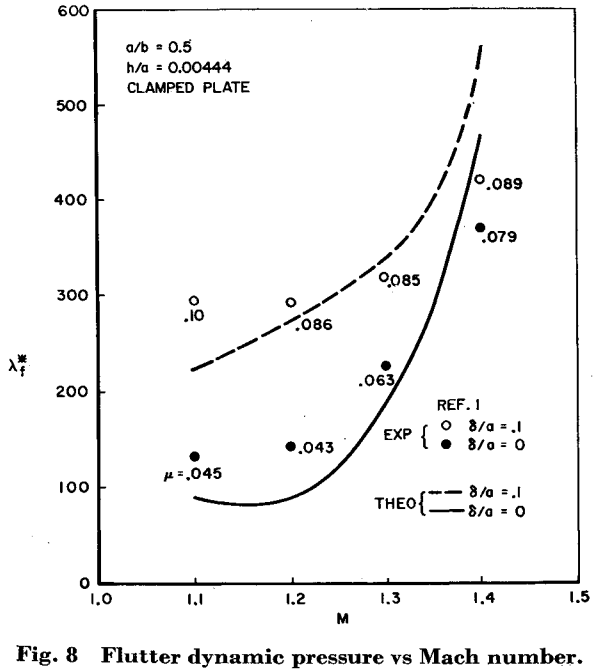

Fig. 8 Flutter dynamic pressure vs Mach number.

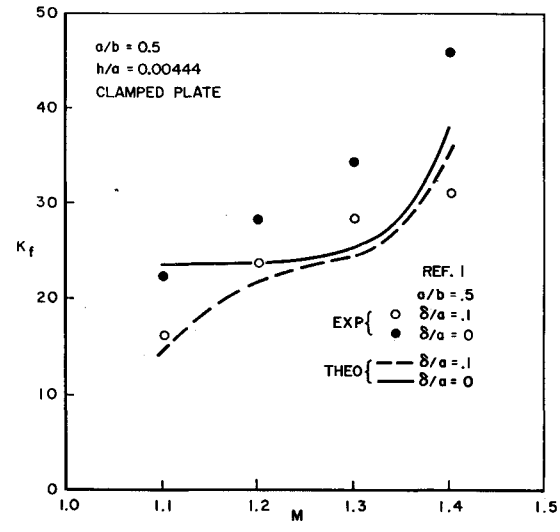

Fig. 9 Flutter frequency vs Mach number.

In Fig. 8 theoretical and experimental results are shown for flutter dynamic pressure vs Mach number with $\delta/a = 0.1$ and 0. Again the $\delta/a = 0$ results are for the first mode flutter rather than the second mode. Figure 9 gives the corresponding flutter frequencies. The results are somewhat less satisfactory for the lowest Mach number, $M = 1.1$, but still quite reasonable. Accounting for the cavity beneath the plate would improve the agreement between theory and experiment slightly (5% or less change in dynamic pressure).

4. Conclusions and Recommendations

1) A theoretical analysis has been carried out for the title problem and shown to be a practical and workable method. 2) The application of the aerodynamic forces in a panel flutter analysis has given theoretical results in reasonable agreement with the available experimental data for the effect of a boundary layer. 3) It is recommended that additional calculations be made over a wider range of parameters, e.g., to compare with the experimental data of Ref. 2. 4) It is recommended that the analysis be extended to include viscosity in the perturbed flow and that a more accurate form of the plate boundary condition be considered. 5) It is further recommended that the capabilities of the basic aerodynamic analysis be exploited to study: a) stabilization of viscous boundary layers by flexible walls; b) sound (pressure) wave propagation through a shear flow, e.g., with applications to noise propagation through jet or boundary layers or sonic boom propagation through a ground shear layer; c) shear layer effects on control surface aerodynamics at supersonic speeds; d) water wave generation by wind.

References

[1] Muhlstein, L., Jr., Gaspers, P. A., Jr., and Riddle, D. W., "An Experimental Study of the Influence of the Turbulent Boundary Layer on Panel Flutter," TN D-4486, March 1968, Ames Research Center, Ohio, NASA.

[2] Gaspers, P. A., Jr., Muhlstein, L., Jr., and Petroff, D. A., "Further Experimental Results on the Influence of the Turbulent Boundary Layer on Panel Flutter," TN D-5798, May 1970, Ames Research Center, Ohio, NASA.

[3] Lock, M. H. and Fung, Y. C., "Comparative Experimental and Theoretical Studies of the Flutter of Flat Panels in a Low Supersonic Flow," AFOSR 670, May 1961, California Institute of Technology, Pasadena, Calif.

[4] Hodson, C. H. and Stocker, J. E., "Commerical Supersonic Transport Panel Flutter Studies," AFFDL RTD TDR-63-4036, May 1964.

[5] Asher, G. W. and Brown, A. W., "Experimental Studies of the Unsteady Aerodynamics of Panels at or Near Flutter with a

Finite Boundary Layer, Mach Number 1 to 10," AFFDL RTD-TDR-63-4268, Dec. 1964, Air Force Flight Dynamics Lab.

[6] Miles, J. W., "On Panel Flutter in the Presence of a Boundary Layer," *Journal of the Aerospace Science*, Vol. 26, 1959, pp. 81–93.

[7] McClure, J. D., "On Perturbed Boundary Layer Flows," Fluid Dynamics Research Lab. Rept. 62-2, MIT, Cambridge, Mass., June 1962.

[8] Anderson, W. J. and Fung, Y. C., "The Effect of an Idealized Boundary Layer on the Flutter of Cylindrical Shells in Supersonic Flow," SM 62-49, California Institute of Technology, Pasadena, Calif., 1962.

[9] Olson, M. D., "On Comparing Theory and Experiment for the Supersonic Flutter of Circular Cylindrical Shells," AFOSR 66-0944, Graduate Aeronatucal Lab., California Institute of Technology, Pasadena, Calif., June 1966.

[10] Zeydel, E. F. E., "Study of the Pressure Distribution on Oscillating Panels in Low Supersonic Flow with Turbulent Boundary Layer," NASA CR-691, Feb. 1967, Georgia Institute of Technology.

[11] Dowell, E. H. and Voss, H. M., "Experimental and Theoretical Panel Flutter Studies in the Mach Number Range of 1.0 to 5.0," AFFDL ASD-TDR-449, The Boeing Co., 1963.

[12] Benjamin, T. B., "Shearing Flow Over a Wavy Boundary," *Journal of Fluid Mechanics*, Vol. 6, Pt. 2, pp. 161–205, 1959.

[13] Landahl, M. T., "On the Stability of a Laminar Incompressible Boundary Layer Over a Flexible Surface," *Journal of Fluid Mechanics*, Vol. 13, 1962, Pt. 14, pp. 609–632.

[14] Graham, E. W. and Graham, B. B., "Effect of a Shear Layer on Plane Waves of Sound in a Fluid," *Journal of the Acoustical Society of America*, Vol. 46, No. 1, Jan. 1969, pp. 169–175.

[15] Miles, J. W., "On the Generation of Surface Waves by Shear Flows. Part 5," *Journal of Fluid Mechanics*, Vol. 30, Pt. I, pp. 163–175, 1967.

[16] Dowell, E. H., "Generalized Aerodynamic Forces on a Flexible Plate Undergoing Transient Motion in a Shear Flow with an Application to Panel Flutter," AIAA Paper 70-76, New York, Jan. 1970.

[17] Liepmann, H. W. and Roshko, A., *Elements of Gas Dynamics*, Wiley, New York, 1957.

[18] Dowell, E. H., "Generalized Aerodynamic Forces on a Flexible Plate Undergoing Transient Motion," *Quarterly of Applied Mathematics*, Vol. 24, No. 4, Jan. 1967, pp. 331–338.

[19] Dowell, E. H., "Nonlinear Oscillations of a Fluttering Plate II," *AIAA Journal*, Vol. 5, No. 10, Oct. 1967, pp. 1856–1862.

[20] Ventres, C. S. and Dowell, E. H., "Comparison of Theory and Experiment for Nonlinear Flutter of Loaded Plates," *AIAA Journal*, Vol. 8, No. 11, Nov. 1970, pp. 2022–2030.

[21] Dowell, E. H., "Theoretical-Experimental Correlation of Plate Flutter Boundaries at Low Supersonic Speeds," *AIAA Journal*, Vol. 6, No. 9, Sept. 1968, pp. 1810–1811.

MAY 1971 AIAA JOURNAL VOL. 9, NO. 5

Jet Aircraft Air Pollutant Production and Dispersion

JOHN B. HEYWOOD,* JAMES A. FAY,† AND LAWRENCE H. LINDEN‡
Massachusetts Institute of Technology, Cambridge, Mass.

In this paper two aspects of pollution from jet engines are considered in detail. Firstly, it is shown that at or near full load, the most important air pollutants are nitric oxide and soot, and the production processes of these two pollutants are then discussed. A kinetic analysis shows that nitric oxide is formed mainly in the combustor primary zone, in regions of the flow where the equivalence ratio is greater than about 0.8, and that freezing occurs as the gas is diluted and cooled in the secondary zone. Calculated results for nitric oxide concentrations in the combustion products are presented and compared with existing experimental data. The mechanisms important in the formation of carbon in the fuel-rich regions of the primary zone are reviewed. The oxidation of this carbon in the remainder of the combustor is then considered, and the oxidation rates attainable within the combustor are computed from existing rate data. Secondly, the dispersion of the exhaust plume in the atmosphere is analyzed, the two effects considered being the entrainment of surrounding air due to turbulent motion of the jet and the motion induced by the buoyancy of the trail. For short times, mixing proceeds as in ordinary wakes; for longer times, mixing is dominated by motion induced by buoyancy.

Introduction

THE production of pollutants in aircraft jet engines and their dissemination in the atmosphere are certainly matters of public concern. A recent survey[1] concludes that "in the vicinities of air terminals, however, the density of pollutant emission by aircraft and the resulting pollutant concentrations are comparable to emission densities and concentrations in adjacent communities of the same pollutants from other sources. Thus, the principal impact of aircraft emissions is local in nature and is expected to become more severe in future years. It is also likely that aircraft emissions will constitute a more significant portion of community-wide pollutant loadings as new aircraft are introduced and as emissions from other sources are reduced." If the emissions from aircraft are averaged over a metropolitan area, their present contribution is insignificant compared with all other sources combined.[2–4] However, aircraft emissions, especially during approach, taxi, and takeoff operations, are confined to a small segment of a metropolitan area and in this respect should be considered a localized source, like a power plant, rather than widely distributed sources, such as automobiles or home heating units. Reference 1 notes that "there are a number of major air terminals at which residential areas are located along an extension of a runway or within a mile or less of the end of the runway. . . . Residents of such an area may ex-

Presented as Paper 70-115 at the AIAA 8th Aerospace Sciences Meeting, New York, January 19–21, 1970; submitted March 16, 1970; revision received December 7, 1970. This research was supported by NASA Grant NGR 22-009-378. The data presented in Fig. 8 were obtained by one of our students, T. Gilmore, and his contribution is gratefully acknowledged.

* Associate Professor of Mechanical Engineering. Member AIAA.

† Professor of Mechanical Engineering. Associate Fellow AIAA.

‡ NSF Fellow. Student Member AIAA.